Indian Journal of Chemical Technology
Vol. 29, January, 2022 pp. 23-31

Magnetic nano carbon balls - Synthesis and adsorption studies

Kumaravelan V[1], Murugesan B[2] & Sivakumar P*[,3]

[1]Department of Chemistry, Kandaswami Kandar's College, Velur, Namakkal 638 182, TN, India.
[2]Department of Chemistry, K. S. R. Institute for Engineering and Technology, Tiruchengode 637 215, TN, India
[3]Department of Chemistry, Arignar Anna Govt Arts College, Namakkal 637 002, TN, India.

E-mail: shivagobi@yahoo.com

Received 30April 2021; accepted 12 August 2021

Madhuca longifolia oil used as precursor oil for the synthesis of nano sized carbon balls with a size of 50 to 100 nm. An indigenously designed reactor assembly is used for this synthesis. Low temperature direct pyrolysis method is employed with the help of multi-metal catalyst derived from *Alternanthera sessilis* stem ash. The synthesized carbon balls have a bulk density of 0.124 g/mL and BET surface area of 805.87 m^2/g. In-order to ensure the effective recovery of NCB, it is immobilized with a magnetic nano particle Fe_3O_4 and used for the adsorption studies of Acid Green 25 dye from aqueous solution under batch mode. Batch mode studies also proved the endothermic nature and physisorption mechanisms. The maximum Langmuir monolayer capacity of 243.90 mg/g has been achieved at a temperature of 45°C.

Keywords: Acid Green 25, *Alternanthera sessilis*, Isotherm, Kinetics, *Madhuca longifolia*

The fast growing human population all around the world exploits the natural resources in a rapid manner. To satisfy the increasing needs of human population, the fresh water resources are exploited. In another way there is a huge quantity of effluents are generated and let out into the water bodies, which also exploits the fresh water bodies. The discharge of these pollutants makes great implications on the human health. Among the different kind of pollutants, dye bearing wastewater are of great concern owing to their high toxicity and non-biodegradable nature. These effluents are released from plastic, paper, cosmetic, and textile industries. There are number of technologies available for the treatment of dye bearing wastewater. Applicability of these technologies is limited owing to the high cost and complicated technologies.

Adsorption using activated materials is a suitable method for the removal of complex organic dye molecules because of its simplicity, high effectiveness, reusability, and ease of process[1]. Several materials like Euphorbia antiquorum (L) wood[2], oil palm trunk fiber[3], pine sawdust[4], carbon developed from Arundodonax root[5], degreased coffee bean[6], bentonite[7], polyurethane foam[8], etc are used as precursor for the preparation of adsorbent.

The objective of the work is to synthesize highly active Nano Sized Carbon Balls (NCB) using *Madhuca longifolia* (Mahuwa) oil with a uniform and average size <100 nm using an indigenous reactor assembly through air controlled, low temperature direct pyrolysis with the help of multi-metal catalyst derived from *Alternanthera sessilis* stem. The synthesized NCB is used for the removal of organic contaminants through adsorption by batch and column mode after immobilizing with Fe_3O_4. The precursor oil for the synthesis of Nano Sized Carbon Balls is derived from the plant *Mahua longifolia*. It is an Indian tropical tree normally found in the forests of central and north India. It belongs to the family Sapotaceae. A matured tree can produce about 20 to 200 kg of seeds. The matured dried seeds are used for the extraction of Mahuwa oil. Mahuwa oil with a fatty acid composition of palmitic 24.5 %, stearic 22.7%, oleic 37.0 %, linoleic 14.3 %[9].

Experimental Section

Materials

All the chemicals used are of analytical grade purchased and used without further purification. All solutions are made using double distilled water.

Preparation of green catalyst

The muti-metal catalyst has been synthesized from the stems of *Alternanthera sessilis.* The air dried stems of *Alternanthera sessilis* are cut into a pieces of

2 to 5 cm length and carbonized in muffle furnace at 750°C for 1 h under constant flow 0.1 bar of nitrogen. The carbonized stem pieces are washed twice with double distilled water, followed by a single alcohol wash and finally dried in a hot air oven at 105°C for 24 h.

Synthesis of NCB

The carbonized stems of *Alternanthera sessilis* are soaked with mahuwa oil for about 30 min and then air dried for about 1h. The air dried, oil soaked stems are kept on a stainless steel grill and it is burnt from the bottom using LPG gas as a fuel mixed with air. The soaked stems start to burn at its ignition temperature, then the fuel gas (LPG) is cut off and the air inlet is regulated in such a way that, the combustion temperature is controlled at 420 to 470°C. The soot formed during the combustion is collected using a dome shaped surface of chromium oxide layer of Stainless steel lid (316SS) which is kept over the combustion chamber. The excess flue gas is allowed to pass through the exhaust vents. The ash formed during the combustion process is frequently removed through the discharge opening provided at the bottom of the reactor. The carbon deposited at the inner surface of Stainless steel dome is carefully collected and washed with double distilled water and finally with alcohol.

Activation of NCB using microwave oven

The carbon balls collected in the above process are stirred with minimum quantity of 4 N nitric acid and made into a paste. The paste is kept in microwave oven and activated at 600w for 5 min. Finally the activated NCB is washed with double distilled water 4 times and an alcohol wash, then dried in a hot air oven for 2 h at 105°C and finally used for further studies.

Synthesis of iron oxide immobilized NCB (Fe_3O_4@NCB)

Exactly 100 mL of 0.1M solution of $FeCl_3.6H_2O$ is mixed with 0.5 g of activated NCB and stirred with magnetic stirrer for about 30 min. Then 1:1 ammonia is added drop wise with this mixture with constant stirring. The gel formation takes place at a *p*H of 8.0. After the gel formation, the ammonia addition is stopped and the contents are continuously stirred for another 4 h. After 4h, the carbon immobilized with Fe is carefully filtered, washed, dried in hot air oven at 110°C for 24h and then finally calcined at 400°C for 1h under constant flow of nitrogen at 0.1 bar. The calcined Fe_3O_4@NCB magnetic composite is cooled to room temperature and stored in tight lid container for further studies.

Characterization

The surface morphology is examined using field emission scanning electron microscope (FE-SEM) ZEISS (Saint Joseph College, Trichy, India) at an accelerating voltage of 5 kV. The HR-TEM image of the NCB is analyzed using Jeol/JEM 2100 instrument at Sophisticated Test & Instrumentation Centre, Cochin University of Science and Technology, Cochin, Kerala, India.

Batch Adsorption studies

Acid Green 25 (AG25) dye (anionic) with a molecular weight of 622.59, formula $C_{28}H_{20}N_2Na_2O_8S_2$, C.I No. 61570 and the absorption maxima at 605 nm, (E. Merck, India) is used as a model solute for the adsorption studies. A stock solution of 1000 mg/L is prepared using appropriate amount of dye dissolved in double distilled water and diluted as and when required. For the batch mode adsorption studies, 100 mL of dye solution of specified concentration is equilibrated with 100 mg of Fe_3O_4@NCB composite in 250 mL tight lid reagent bottle (Borosil-R glass bottles) using REMI make orbital shaker. For the effect of *p*H, 1M HCl and 1M NaOH solutions are used to adjust the *p*H of the solution. After the specified time of agitation, the contents of the flask are centrifuged using universal make centrifuge at 5000 rpm and the final concentration of the dye solution is estimated by measuring the absorbance at the λmax of the dye solution (605 nm) using UV-VIS spectrometer (Model: Elico-BL198). All the adsorption experiments have been done in duplicated and the maximum deviations from the two runs are 4% only.

The percentage and amount of dye removed through adsorption is calculated using the following relationships.

Percentage of dye removed =

$$\frac{Intial\ concentration(C_0) - Concentration\ at\ time\ t\ (C_t)}{Initial\ concentration\ (C_0)} \times 100 \quad \ldots (1)$$

Amount of dye removed per unit weight of adsorbent (q_t)

$$= (C_0 - C_t)\frac{V}{W} \ \text{mg/g} \quad \ldots (2)$$

Where, V is the volume of dye solution in mL and W is the weight of adsorbent in grams

Results and Discussion

Surface characteristics of the NCB and Fe_3O_4@NCB

During the combustion of Mahuwa oil, nano sized carbon balls are deposited at bottom surface of the SS dome. The synthesized carbon is washed with distilled water and the surface topography is tested using SEM images. The SEM images (Fig. 1a) of pure carbon indicated that the nano carbon balls with extremely uniform size of 40 to 80nm are formed. The SEM images of the Fe immobilized on NCB (Fe_3O_4@NCB) is shown in Fig 1b. There is a uniform distribution of Fe_3O_4 on the surface of carbon without much agglomeration. All the NCB are of spherical and uniform in size. The smaller size nano carbon balls give large surface area as indicated from the BET surface area analysis studies (Table 1). The immobilization of Fe slightly reduces the total surface area, where as this can be compromised with other advantages like, increased bulk density and magnetic behavior. The lower bulk density values indicate that, the synthesized carbon balls and very small in size with some hollowness inside the balls[10]. This lower density also indicates the high surface to bulk volume of the synthesized NCB.

The HR-TEM images were recorded to ascertain whether the carbon balls are solid of hollow spheres. The TEM image in Fig. 2 indicated that the carbon balls are solid spheres with 50 to 90 nm diameter. The fringes on the carbon surface indicated the graphitic type of carbon layers stacked together and makes the solid carbon spheres.

Influence of Solution *p*H

To evaluate the role of solution *p*H onto the adsorption of AG25 on the surface of Fe_3O_4@NCB, the adsorption experiments were performed by adjusting the solution *p*H from 2.0 to 12.0. As observed from the plot of solution *p*H vs percentage of AG25 removal (Fig. 3), the dye adsorption is high when the solution *p*H is kept low and it showed a

Table 1 — Physico-chemical properties of NCB and Fe_3O_4@NCB

S.No	Property	NCB	Fe_3O_4@NCB
1.	*p*H	6.9	7.4
2.	pH_{ZPC}	6.6	7.1
3.	Bulk Density, g/mL	0.124	0.221
4.	BET Surface Area, m^2/g	805.87	774.08
5.	Moisture content, %	8.71	9.12
6.	Volatile matter, %	3.34	3.26

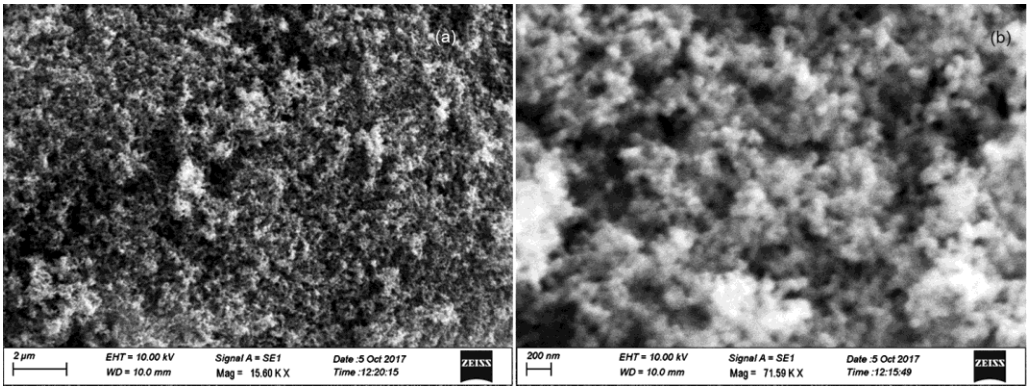

Fig. 1 — SEM images a) NCB and b) Fe_3O_4@NCB

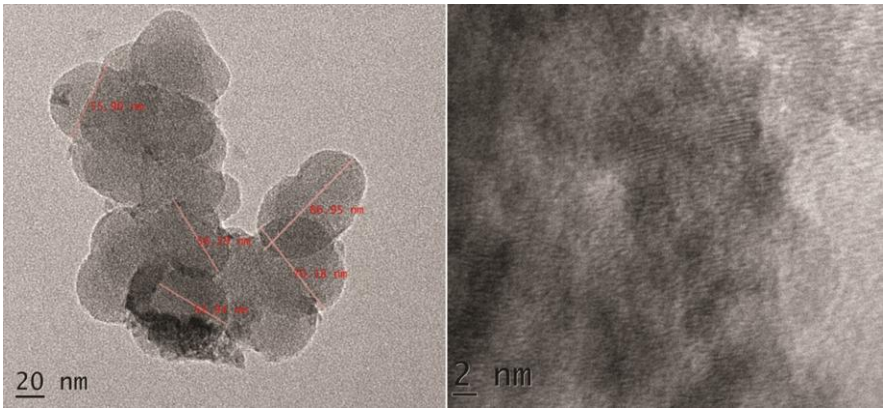

Fig. 2 — HR-TEM images NCB

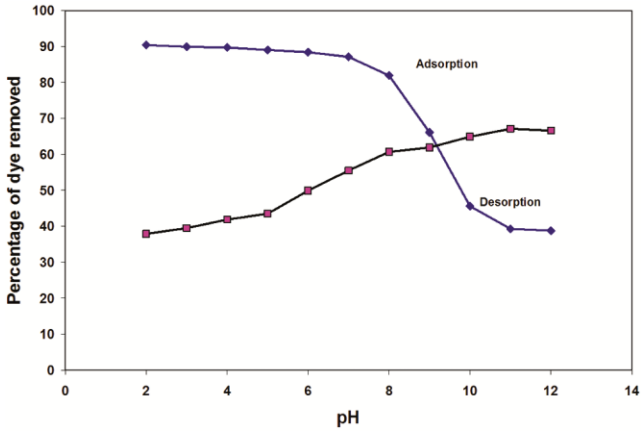

Fig. 3 — Effect of *p*H on the adsorptive removal of AG25

decreasing trend at high *p*H. The percentage of AG25 removed at a *p*H of 2.0 is 90.4% and it slightly decreased upto a *p*H of 7.0 (87.1%). When the solution *p*H exceeds 7.0, there is a drastic decrease in the adsorption and finally at a *p*H of 12.0, the adsorptive removal of AG25 decreased to 38.8%.

The dye AG25 is an anionic dye, it ionises into $AG25^{2-}$ and $2Na^{+}$ in aqueous solution as shown in Fig. 4. In the lower *p*H, the surface of the adsorbent is protonated and becomes positively charged. The positively charged Fe_3O_4@NCB surface will attract the negatively charged dye anion and thereby the system shows an enhanced adsorption at lower *p*H. When the *p*H of system reaches 7.0, the Vander Waals forces of attraction is predominant rather than the ionic attraction. The moderate dye removal at the intermediate *p*H range is mainly due to weak attractions and pore diffusions.

When the solution *p*H exceeds 7.0, the surface of sorbent becomes negative. The negatively charged sorbent surface will repel the anionic dye molecule. This sort is repulsive force caused by the like charge surface and dye ions will decrease the amount of dye adsorption onto the surface of Fe_3O_4@NCB. Literature review substantiated the similar kind of variation for the adsorption of coomassie brilliant (CB) blue R-250 anionic dye adsorption onto nano-hydrogel prepared from starch/poly (alginic acid-*cl*-acrylamide[11]. The desorption of the dye loaded adsorbent is also analysed and presented in the Fig. 3. High percentage of dye desorbed at higher *p*H. Dilute NaOH can be suitable eluent for the effective regeneration of spent Fe_3O_4@NCB composite.

Influence of dye concentration

The initial dye concentration has great influence in the determination of maximum sorption capacity

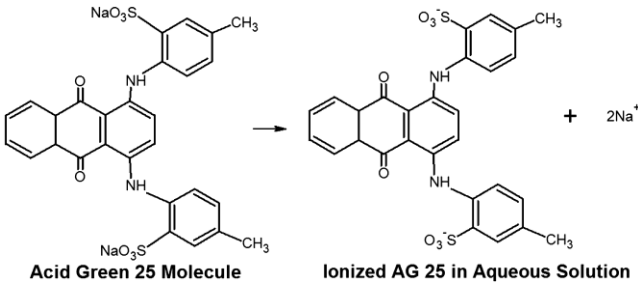

Fig. 4 — Ionization of Acid Green 25 in aqueous solution

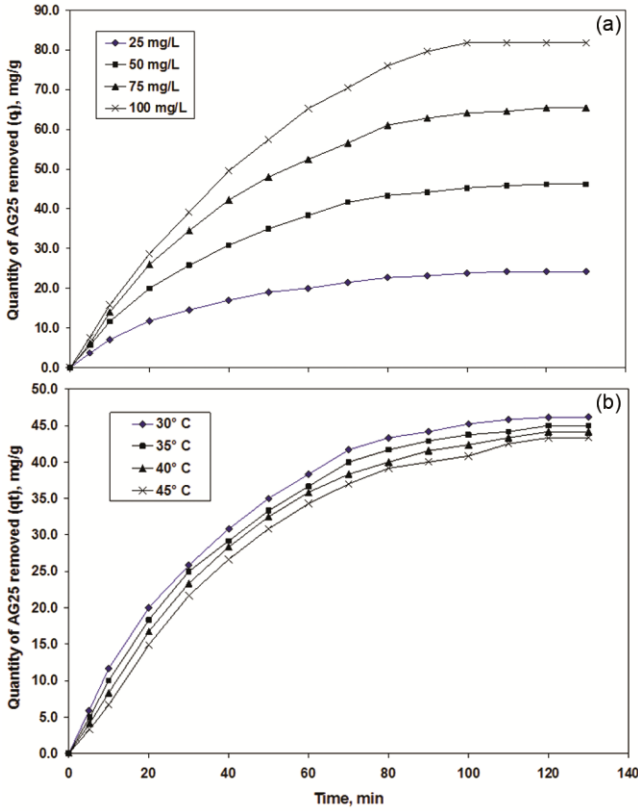

Fig. 5 — Variation of AG25 adsorption onto Fe_3O_4@NCB. a) Effect of Initial AG25 concentration and b) Effect of temperature

of any adsorbing material[12]. In the present study, adsorption experiments are performed for a fixed AG25 concentration of 25, 50, 75 and 100 mg/L. As observed from the Fig. 5a, the AG25 adsorption by Fe_3O_4@NCB increased from 24.22 to 81.77 mg/g on increasing the initial AG25 concentration from 25 to 100 mg/L. At the beginning of adsorption process, the rate of adsorption is very high when compared with that of rate of desorption. This is the reason behind the steep increase of the adsorption curve at the beginning. The active sites available for the solute molecules decreases during the progression of

adsorption therefore the rate of adsorption also decreases. When the time progresses, the rate of adsorption decreases and the rate of desorption increases, lead to slow uptake of AG25. After 120 min of agitation, the rate of adsorption is equal to rate of desorption, means the adsorption reached equilibrium. This gives an idea that the adsorption of AG25 by Fe_3O_4@NCB reaches equilibrium in 120 min.

Only the total quantity of AG25 removed per unit mass of adsorbent increases proportionally with AG25 concentration, but the percentage removal of AG25 decreases with increase of AG25 concentration. At high solute concentrations, the number of sorption sites available per unit quantity of solute molecule (in this case AG25) decreases which ultimately results in low percentage of dye removal. For an effective adsorption, the active surface sites are highly essential, which are less at higher concentration[13,14].

Influence of system temperature

System temperature is also a dominant factor for the effective adsorptive removal of a solute from its solution. The variation of AG25 adsorption by Fe_3O_4@NCB at different temperatures is ascertained and presented graphically in Fig. 5b. The amount AG25 removed by Fe_3O_4@NCB decreased from 46.17 to 43.33 mg/g on increasing the system temperature from 30 to 45°C for a fixed initial AG25 concentration of 50mg/L. The decrease of adsorption of AG25 with respect to increase of system temperature indicated the exothermic nature. The heat release during the adsorption will inflate desorption rate, there by the quantity of AG25 removed per unit mass of Fe_3O_4@NCB decreased on increasing the temperature. The adsorbed species will acquire more kinetic energy at high temperatures, thereby the affinity with the sorbent surface breaks and the solute will get less adsorption at high temperature. Generally weekly bound solute molecules tent to desorb at high temperatures, substantiated the physisorption nature of AG25 adsorption onto Fe_3O_4@NCB.

Adsorption kinetics

The adsorption of a solute molecule by an adsorbent is influenced by various environmental factors and for a fixed condition the adsorption follows different mechanisms. The properties of solute and sorbent will be the key factor for the adsorption kinetics. The study of adsorption kinetic is essential for the effective treatment of industrial effluents using high surface nanomaterials. As the kinetic studies provides essential information about the reaction pathways and the sorption mechanism. The prestated kinetic models like pseudo-first order[15], pseudo-second order[16], Elovich[17] and Intra-particle diffusion kinetic models[18]were employed to study the mechanism of adsorption and the rate limiting step[19].

The linear form of these kinetics models are:

Pseudo-first order model: $\log(q_e - q_t) = \log q_e - \frac{k_1}{2.303} t$ … (3)

Pseudo-second order model: $\frac{t}{q_t} = \frac{1}{k_2 q_e^{\,2}} + \frac{1}{q_e} t$ … (4)

Elovich kinetic model: $q_t = \frac{1}{\beta} \ln(\alpha\beta) + \frac{1}{\beta} \ln(t + t_0)$ … (5)

Intra-particle diffusion model: $q_t = k_d \cdot t^{1/2}$ … (6)

Pseudo-first order and pseudo-second order kinetics

In the case of liquid phase adsorption, rate law is derived based on the rate limiting step (slowest among all steps)[20]. Generally, the pseudo first order kinetic model is employed to describes the adsorption at the beginning of the adsorption process, whereas the pseudo-second order model is used describe the entire range adsorption[19]. The results of kinetic data analysis are presented in Table 2. When the kinetics data for the adsorption of AG25 onto Fe_3O_4@NCB analysed using the pseudo first order expression, the results indicated that the pseudo first order rate constant 3.593×10^{-2} to 4.076×10^{-2} min^{-1} for the under different initial AG25 concentrations. The same rate constant varies from 3.270×10^{-2} to 3.593×10^{-2} min^{-1} under the range of temperatures investigated. As the data collected over the entire period of adsorption is analysed using the pseudo first order expression, but the pseudo first order expression hold good during the initial stages of adsorption. This is the reason for the deviation of pseudo first order expression for the AG25 onto Fe_3O_4@NCB.

When the adsorption data analysed using the pseudo second order expression, the second order rate constant k_2 decreases from 1.359×10^{-3} to 0.155×10^{-3} g/mg/min on increasing the AG25 concentration from 25 to 100 mg/L and it decreases from 5.226×10^{-4} to 2.368×10^{-4} g/mg/min on increasing the temperature from 30 to 45° C. At high concentration, the number of AG25 molecules competing for the sorbent surface is more and at the same time the number of molecules in the adsorbed phase is also high, therefore this will

Table 2 — Results of kinetic plots

Parameters	Initial dye concentration, mg/L				`Temperature, ℃			
	25	50	75	100	30	35	40	45
$q_e$exp.(mg/g)	24.22	46.17	65.41	81.74	46.17	45.00	44.17	43.33
Pseudo first order kinetics								
$k_1 \times 10^{-2}$ (min^{-1})	3.685	4.076	3.869	3.593	4.076	3.593	3.362	3.270
$q_e$cal(mg/g)	27.75	62.27	88.57	106.39	62.27	55.54	52.83	54.36
r^2	0.9661	0.9586	0.965	0.9326	0.9586	0.9839	0.9843	0.9752
Pseudo second order kinetics								
$k_2 \times 10^{-4}$(g/mg/min)	13.59	5.10	2.51	1.55	5.10	4.379	3.458	2.368
h	1.1623	1.81	2.07	2.31	1.81	1.57	1.33	1.08
$q_e$cal(mg/g)	29.24	59.52	90.91	121.95	59.52	59.88	62.11	67.57
r^2	0.9517	0.9174	0.8536	0.813	0.9174	0.8829	0.8358	0.7249
Elovich model								
α (mg g^{-1} min^{-1})	10.60	23.73	37.36	47.91	23.73	21.30	22.06	23.07
β (g mg^{-1})	0.1746	0.0893	0.0625	0.0508	0.0893	0.0976	0.1000	0.1027
r^2	0.9585	0.941	0.9265	0.8895	0.941	0.9091	0.8949	0.8741
Intra particle diffusion model								
k_{id}(mg/g/$min^{½}$) Film diffusion	0.3634	0.2068	0.1545	0.1381	0.2068	0.2163	0.2322	0.2524
r^2	0.9713	0.9576	0.9358	0.9418	0.9576	0.939	0.9199	0.894
k_{id}(mg/g/min½) Pore diffusion	0.6358	0.3204	0.1980	0.1360	0.3204	0.3156	0.3223	0.3080
r^2	0.9737	0.9334	0.9459	0.9469	0.9334	0.9324	0.9652	0.9600

tent to desorb from the surface and thereby reduces the rate constant of the adsorption. High temperature increases the kinetic energy of the molecules, which enhances desorption and there by shifts the adsorption equilibrium towards the left side, which will reduce the rate constant of the adsorption kinetics. Under the given set of operating conditions, the correlation coefficient for pseudo first order kinetics is more than pseudo second order kinetics. On analysing the adsorption profile Fig. 5a and 5b, the adsorption was rapid during initial phase of adsorption and major portion of adsorption completed during the initial 30 min. More adsorption in the initial period will reflect the high degree of fitness for the pseudo first order kinetics than pseudo second order kinetics.

Elovich kinetics

Elovich kinetic model is not related to mechanism of adsorption, it is derived to evaluate the nature of adsorption. The model was proposed by Roginsky and Zeldovichin (1934) for the chemisorption type of adsorptions[21]. This model is successfully applied for systems having slow adsorption and systems with heterogeneous adsorbing systems. The parameter α (initial rate of adsorption) increases from 10.60 to 47.91 mg/g/min on increasing the concentration from 25 to 100 mg/L and it increases from 20.69 to 23.07 mg/g/min on increasing the system temperature from 30 to 45° C. The higher population of solute molecules at high concentration increases the driving force and there by the accumulation of solutes on the sorbent surface increases with concentration. Another parameter β (related to the extent of surface coverage) decreases with increase of AG25 concentration and increases with increase of solution temperature. The data fitted reasonable well for the Elovich model, indicated that chemisorption also plays a significant role and the surface also energetically heterogeneous.

Intraparticle diffusion model

This model proposed by Weber and Morris **(**1963) is a widely used model to predict the mechanism involved during the rate controlling step[18]. Generally the liquid stage adsorption proceeds in four steps. The first step is the migration of solute from bulk of the solution to the vicinity of adsorbent and concentrates around the adsorbent. The second step is the diffusion of solute through the boundary layer onto the surface of adsorbent and forms a thin film (called as film diffusion). Third step is the penetration of the solute molecules into the interior pores of the adsorbent (called as pore diffusion). The fourth and final step is adsorption of the adsorbate on the surface of adsorbent. Among the four steps, the second and third steps are the slow and rate limiting steps as the other two steps are fast[22]. In this individual rate constants

for these two steps were determined and analysed. Based on the results of individual steps, there is no much deviation was observed between these steps in terms of r^2 and k_{ID}, therefore it is imperative that both film diffusion (due to surface functionalities) and pore diffusion (due to the porosity of carbon) are operating simultaneously.

Adsorption Isotherm

Adsorption isotherm gives a relationship between the concentrations of solute of the sorbent surface to that of in solution. The isotherm studies provide some useful information about the surface properties (energetically homogeneous/heterogeneous), mechanism of adsorption and it also provides some knowledge about the adsorbate-adsorbent interaction[23]. Langmuir (1918)[24] and Freundlich (1906)[25] isotherm models are frequently employed for the analysis of adsorption isotherm in liquid phase adsorption. The linear form of Langmuir and Freundlich models are:

$$\text{Langmuir model: } \frac{C_e}{q_e} = \frac{1}{Q_0.b_L} + \frac{C_e}{Q_0} \quad \ldots (7)$$

Freundlich Model:

$$\log q_e = \log k_f + \frac{1}{n}\log C_e \quad \ldots (8)$$

Langmuir isotherm derived with an assumption that the surface of adsorbent is energetically homogeneous, the adsorbent forms monolayer on the surface of adsorbent and there is no interaction between the adsorbed molecules[26]. The Langmuir plot for the adsorption of AG25 onto Fe_3O_4@NCB is shown in Fig. 6a and the results calculated based on this model are presented in Table 3. The maximum adsorption capacity of Fe_3O_4@NCB for the adsorption of AG25 (with an assumption of monolayer adsorption) increases from 192.31 to 243.90 mg/g on increasing the solution temperature from 30 to 45°C. This is comparable with that of the values reported by the past researchers for the adsorption of AG25 onto various adsorbents (Table 4). The dimensionless parameter R_L varied between 0 and 1 indicated the favourability of adsorption under given set of operating parameters.

The adsorption isotherm data is also analysed using Freundlich adsorption isotherm as indicated in the Fig. 6b and results generated are presented in Table 3. The Freundlich model is derived with an assumption that the accumulation of solute on the surface of sorbent increases proportionally with concentration. The Freundlich parameter n varies between 3.46 to 1.64, indicated the favourability of adsorption for the selected adsorbent-adsorbate system. The correlation coefficient (r^2) for the Freundlich model is little higher than Langmuir model, substantiated the surface heterogeneity of Fe_3O_4@NCB composite adsorbent. Freundlich model is more appropriate to describe the adsorption of AG25 with high r^2 value.

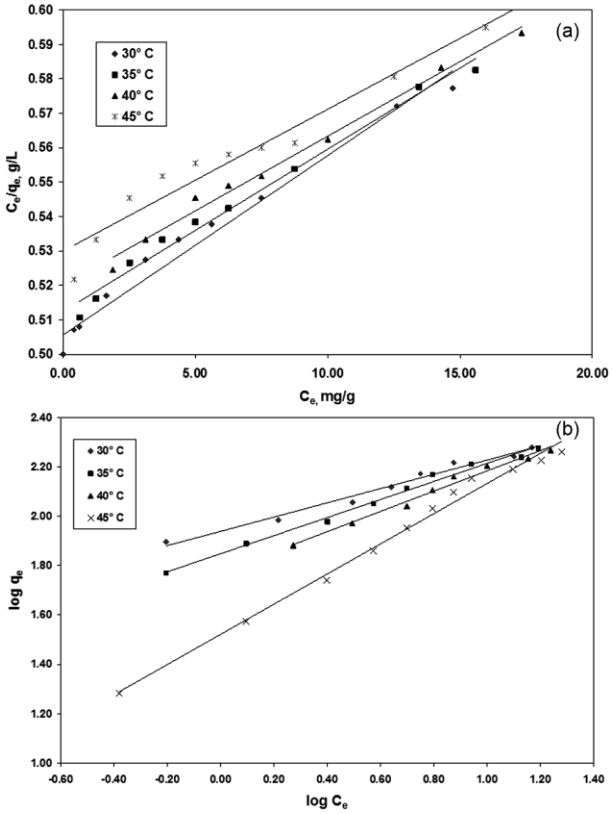

Fig. 6 — a) Langmuir plot for the adsorption of AG25 onto Fe_3O_4@NCB and b) Freundlich plot for the adsorption of AG25 onto Fe_3O_4@NCB

Table 3 — Results of Isotherm analysis for the adsorption of AG25 onto Fe_3O_4@NCB

Parameters	Temperature °C			
	30	35	40	45
Langmuir isotherm				
Q_0 (mg/g)	192.31	212.77	232.56	243.90
b_L (L/mg)	0.0103	0.0092	0.0083	0.0077
r^2	0.9777	0.9874	0.9906	0.9442
R_L	0.469 to 0.928			
Freundlich isotherm				
n	3.46	2.73	2.43	1.64
k_f ($mg^{1-1/n}\ L^{1/n}\ g^{-1}$)	86.88	70.53	59.31	33.20
r^2	0.9808	0.9902	0.9841	0.9902

Table 4 — Langmuir monolayer adsorption capacity of AG25 onto various adsorbents

S. No	Adsorbent	Q_0, mg/g	Reference
1.	Polyaniline nanotubes salt/silicacomposite	6.89	27
2.	Ananas Comosus (L) Activated carbon	303.03 to 357.14	28
3.	Surfactant modified-bentonite	2.98 to 3.72	29
4.	Protonated chitosan	320.5 and 300.5	30
5.	Oxidized Multi-Walled Carbon Nanotubes	333.0	31
6.	Shells of bittim (Pistaciakhinjuk Stocks)	7.0 to 16.0	32
7.	Quaternizedkenaf core fiber	344.83	33
8.	Fe_3O_4@NCB	192.31 to 243.90	Present study

Adsorption Thermodynamics

There are different method employed for the estimation of thermodynamic parameters like ΔG (Gibbs free energy), ΔH (Enthalpy of adsorption) and ΔS (Enthalpy of adsorption). The first method is the use of Langmuir equilibrium constant as per the following equation

$$\Delta G = -RTlnb_L \quad \ldots (9)$$

Where, b_L is the Langmuir equilibrium constant. According to Liu (2009), calculation of thermodynamic parameters using Langmuir equilibrium constant is valid for adsorbent with less charge and also for diluted solutions of adsorbate[34]. In the present study, the carbon surface does not have much functionality and also the AG25 solutions used in this study are also less than 100 mg/L. Based on these facts, the Langmuir equilibrium constant is used for the calculation of the above stated thermodynamic parameters and the results are given in Table 5. The negative Gibbs free energy specified the spontaneity of the adsorption of AG25 onto Fe_3O_4@NCB. The enthalpy and entropy of the adsorption are calculated using the following expression.

$$\Delta G = \Delta H - T\Delta S \quad \ldots (10)$$

Combining the above equations

$$lnb_L = -\frac{\Delta H}{RT} + \frac{\Delta S}{R} \quad \ldots (11)$$

Where, T is the system temperature in Kelvin scale.

The Enthalpy and Entropy of the adsorption are calculated from the slope and intercept of the plot of lnb_L *vs* 1/T respectively (Figure 7).

The negative value of enthalpy of adsorption proves that the adsorption decreases and desorption increases on increasing the system temperature. During the adsorption the solute molecules in the solution will accumulate on the sorbent surface and thereby the randomness in the solution decreases and orderliness increases.

Table 5 — Thermodynamic parameters for the adsorption of AG25 onto Fe_3O_4@NCB

Temperature, °C	ΔG, kJ/mol	ΔH, kJ/mol	ΔS, J/K/mol
30	- 4.678		
35	- 4.462	- 15.373	- 35.37
40	- 4.264		
45	- 4.156		

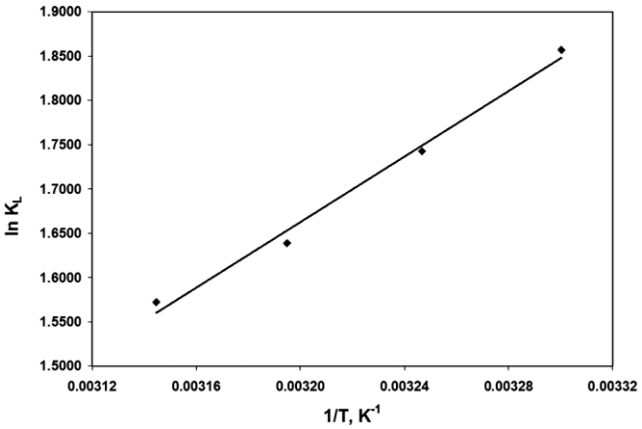

Fig. 7 — Van't Hoff plot for the Adsorption of AG25

Conclusion

Nano Sized Carbon Balls (NCB) with a uniform size of 50 to 100 nm are successfully synthesized by chemical vapour deposition using *Madhuca longifolia* oil as a precursor oil. The strings of Nano Sized Carbon Balls (NCB) formed over the surface of multi-metal catalyst derived from *Alternanthera sessilis* stem ash. The magnetically immobilized NCB has great potential for the removal of Acid Green 25 dye under batch mode of adsorption. SEM and HR-TEM studies revealed the structure of NCB and its surface topography. Kinetic studies proved that the composite follows pseudo-first order during the beginning of adsorption and later it deviates to pseudo-second order. Analysis of isotherm data using Langmuir and Freundlich adsorption isotherms demonstrated the adsorption mechanism. Exothermic and spontaneous nature of adsorption is proved by the thermodynamic

studies. The study proved that the synthesized composite is a good adsorbent for textile dyes.

References

1 Naushad M & Alothman Z A, *Desalin Water Treat*, 53 (2015) 2158.
2 Sivakumar P & Palanisamy P N, *J Sci Indus Res*, 68 (2009) 894.
3 Hameed B & El-Khaiary M, J *Hazard Mater*, 154 (2008) 237.
4 Witek-Krowiak A, *Desalin Water Treat*, 51 (2013) 3284.
5 Zhang J, Li Y Zhang C & Jing Y, *J Hazard Mater*, 150 (2008) 774.
6 Baek M H, Ijagbemi C O, Se-Jin O &Kim D S, *J Hazard Mater*, 176 (2010) 820.
7 Bulut E, Ozacar M & Sengil A S, *Microporous Mesoporous Mater*, 115 (2008) 234.
8 Leite B T, Robaina N F, Reis L G T D, Netto A D P & Cassella R J, *J Cassella Water Air Soil Pollut*, 223 (2012) 1303.
9 Trifed, "Product profile Mahuwa Ministry of Tribal Affairs Government of India"*Trifednicin Retrieved*, Please tell me volume number (2013) 11
10 Murugesan B, Sivakumar A, Loganathan A & Sivakumar P, *J Taiwan Inst Chem Eng*, 71 (2017) 364.
11 Sharma G, Naushad Mu Kumar A, Rana S, Sharma S, Bhatnagarc A, Stadler F J, Ghfar A A & Khan M R, *Proc Safety Environ Protec*, 109 (2017) 301.
12 Palanisamy P N & Sivakumar P, *Desalin*, 249 (2009) 388.
13 Fu F & Wang Q, *J Environ Manage*, 92 (2011) 407.
14 Naushad M, Vasudevan S, Sharma G, Kumar A L & Othman Z A, *Desalin Water Treat*, 57 (2016) 18551.
15 Langergen S & Svenska B K, *Veteruskapsakad Handlingar*, 24 (1898) 1.
16 Ho Y S & Mckay G, *Proc Biochem*, 34 (1999) 451.
17 Vaghetti J C P, Lima E C, Royer B, da Cunha B M, Cardoso N F, Brasil J L &Dias S L P, *J Hazard Mater*, 162 (2009) 270.
18 Weber W J & Morris J C, *J Sanitary Eng Div Am Soc Civil Eng*, 89 (1963) 31.
19 Magdy Y H & Altaher H, *J Environ Chem Eng*, 6 (2018) 834.
20 Liu Y & Liu Y J, *Sep Purif Technol*, 61 (2018) 229.
21 Roginsky S Z & Zeldovich J, *Acta Physico Chim USSR*, 1 (1934) 554.
22 Altaher H, Khalil T E & Abubeah R, *Color Technol*, 130 (2014) 205.
23 Lima E C, Adebayo M A & Machado F M, ISBN 978-3-319-18874-4 Springer, 33 (2015) 69.
24 Langmuir I, *J Am Chem Soc*, 40 (1918) 1361.
25 Freundlich H M F, *Z Phys Chem*, 57 (1906) 385.
26 Leechart P, Nakbanpote W & Thiravetyan P, *J Environ Manage*, 90 (2009) 912.
27 Ayad M M & El-Nasr A A, *J Nanostructure Chem*, 3 (2012) 2.
28 Parimalam R, Raj V & Sivakumar P, *E-J Chem*, 9 (2012) 1683.
29 Koswojo R, Utomo R P, Ju Y, Ayucitra A, Soetaredjo Z E, Sunarso J & Ismadji S, *App Clay Sci*, 48 (2010) 81.
30 Gibbs G, Tobin J M & Guibal E, *J App Polymer Sci*, 90 (2003) 1073.
31 Sobhanardakani S & Zandipak R, *Iranian J Health Sci*, 3 (2015) 48.
32 Aydın H& Baysal G, *Deslin*, 196 (2006) 248.
33 Idan I J, Abdullah L C, Choong T S Y, Nurul S & Md Jamil A B, *Ads Sci Technol*, 36 (2018) 1.
34 Liu Y, *J Chem Eng Data*, 54 (2009) 1981.